Original Article

Antitumor effects of artesunate on human breast carcinoma MCF-7 cells and IGF-IR expression in nude mice xenografts

Hai-Ying Dong[1], Zhi-Fei Wang[2]

[1]Department of Oncology, Zhejiang People's Provincial Hospital, Hangzhou 310014, China; [2]Department of Hepatobiliary and Pancreatic Surgery, Zhejiang People's Provincial Hospital, Hangzhou 310014, China

Correspondence to: Zhi-Fei Wang. Department of Hepatobiliary and Pancreatic Surgery, Zhejiang People's Provincial Hospital, Hangzhou, China. Email: zhifei1973@126.com.

Purpose: The objective of this study was to investigate the anti-tumor effects and analyze the mechanism of artesunate (ART) action on breast cancer *in vivo* using tumor transplanted nude mice.

Methods: The human breast tumor cell line MCF-7 was transplanted into nude mice, and the animals were treated with various doses of ART alone or in combination with cyclophosphamide (CTX) or normal saline (NS). The tumor inhibitory effects were observed and compared, and the ultrastructural morphology of the transplanted tumor cells was observed by electron microscopy. The apoptosis rates and cell cycle status were detected by flow cytometry (FCM). The expression of apoptosis-related proteins p53, Bcl-2, Bax and Caspase-3 were detected by immunohistochemistry and IGF-IR was detected by western blot. The expression correlation for these proteins was also analyzed.

Results: The tumor inhibition rates in the low dose ART group, high dose ART group, CTX group and combined drug therapy group were (24.39±10.20)%, (40.24±7.02)%, (57.01±5.84)% and (68.29±5.1)%, respectively. The cell cycle was arrested in phase G_0/G_1 after treatment with ART. The expression of Bcl-2 was significantly reduced, and the expression levels of Bax and Caspase-3 were significantly increased in the ART group compared to the negative control saline group. There was no significant difference detected in p53 expression. The Bcl-2 level was negatively related to Bax and Caspase-3. The western blotting results showed IGF-IR downregulation.

Conclusions: ART inhibits the growth of MCF-7 breast tumor cell xenografts in nude mice. The anti-tumor mechanism of ART for human breast carcinoma in nude mice might be correlated with the alteration of apoptosis related protein expression, which may further induce apoptosis and inhibit cell proliferation.

Keywords: Artesunate (ART); nude mice; anticancer effect; cell apoptosis

Submitted Feb 08, 2014. Accepted for publication Feb 22, 2014.
doi: 10.3978/j.issn.1000-9604.2014.04.07
View this article at: http://www.thecjcr.org/article/view/3698/4576

Background

Traditional Chinese medicine is one of the important resources for the development of modern drugs. Artemisinin (ARS) is the active component of the Chinese medicinal herb *Artemisia annua L*. Its analogues, including dihydroartemisinin (DHA), artesunate (ART) and artemether (ARM), have been used extensively as anti-malarial drugs worldwide and have recently been suggested to have antitumor effects (1-5).

Many studies have examined the antitumor effects of ARS and its derivatives in addition to its anti-malarial effects. ARS inhibits many tumor cell lines *in vitro*, and there is no cross-drug resistance with traditional chemotherapeutic drugs. Lai *et al*. reported oral ARS significantly delayed the development of breast tumors. The number of breast tumors in ARS-fed rats was significantly reduced, and the tumors were smaller in size than the controls. DHA induces apoptosis in HL-60 leukemia cells in an iron and p38 mitogen-activated protein kinase activation dependent manner. However, the mechanism is independent of reactive oxygen species (6). It was

demonstrated that DHA potently inhibits the growth of ovarian cancer cells and *in vivo* tumors. Additionally, DHA enhances the therapeutic effects of carboplatin (CBP) both *in vitro* and *in vivo* by increasing apoptosis (7,8). ART attenuates the growth of human colorectal carcinoma and inhibits hyperactive Wnt/beta-catenin signaling (9). Our previous studies have demonstrated ART can inhibit the growth of Hela and K562 cells *in vitro* (10,11). However, few studies investigating the anti-tumor effects of ART *in vivo* have been reported. Furthermore, the mechanisms of action for the anti-tumor activities are not fully understood. The mechanism may be associated with selective cytotoxicity of cancer cells (12), induction of apoptosis (5,7,8), modulation of gene expression (9,13), cell cycle arrest (14) and inhibition of angiogenesis (15). We established a xenograft model of MCF-7 breast tumor cells by percutaneous injection into nude mice. We observed the antitumor effects of ART and investigated its mechanisms of action. These studies may provide the biological basis for using ART as an anti-tumor therapy.

Materials and methods

Tumor cell lines and experimental animals

The human breast cancer cell line MCF-7 was provided by the Tumor Research Institute of Heilongjiang Province, China. Twenty-five female BALB/c nude mice, aged 3-4 weeks with weight of 13-16 g were purchased from Beijing victory Unilever laboratory animal technology and used for experiments. The animals were housed and fed for one week in a specific pathogen free (SPF) environment.

Reagents and instruments

ART was provided by Guilin Pharmaceutical Co., Ltd., China. The compound was dissolved in $NaHCO_3$ and diluted with saline to the desired concentration. Cyclophosphamide (CTX) was purchased from Jiangsu Hengrui Medicine Co., Ltd., China, and diluted with saline to the desired concentration before use. RPMI-1640 medium was obtained from Gibco Corporation. Propidium iodide (PI) was purchased from Sigma Corporation, USA. Rabbit anti-mouse BCL-2 antibody, mouse Bax monoclonal antibody, rabbit anti-mouse Caspase-3 monoclonal antibody, and the mouse p53 monoclonal antibody were purchased from Wuhan Boster bio-engineering limited company, China. The insulin-like growth factor-I receptor (IGF-IR) monoclonal antibody was purchased from Santa Cruz (USA). The immunohistochemistry kit SP-9001/SP9002 was purchased from Beijing Zhongshan Biotechnology Limited Company, China. The western blot system and enhanced chemiluminescence (ECL) reagent were purchased from Amersham Pharmacia Biotech, USA.

Cell culture and nude mice experiments

MCF-7 cells were cultured in Minimum Essential Eagle's Medium supplemented with 10% fetal bovine serum (FBS), 100 U/mL of penicillin and 100 μg/mL of streptomycin at 37 ℃ in a 5% carbon dioxide (CO_2) atmosphere. The cells were cultured in the logarithmic growth phase, and a single cell suspension at a density of 1×10^7/mL was prepared. The cell suspension was subcutaneously injected (1×10^7/mL in 200 μL PBS) into the right flank of the nude mice. The tumors grew to approximately 3 mm^3 after 8 days. The animals were then divided randomly into the following five groups: a normal saline (NS) group as negative control, low dose of ART group (100 mg/kg), high dose of ART group (200 mg/kg), CTX (40 mg/kg) group as a positive control and combined drug therapy group (CTX + high dose of ART). CTX was administered via intraperitoneal injection while saline and ART were delivered by intragastric administration at a dose of 0.2 mL per mouse daily. The growth status of implanted tumors was observed before and after drug administration. The mice were sacrificed after 12 days of continuous drug administration. The tumors were removed, and tumor size and animal body weight were measured. The tissues were divided into four parts for the following studies: one part for ultrastructural morphology observation of transplanted tumor cells by electron microscope, one part for analysis of the apoptosis rates and cell cycle by FCM, one part for detection of apoptosis related proteins p53, Bcl-2, Bax, Caspase-3 and IGF-IR by immunohistochemistry, and one part of the tissues were frozen in liquid nitrogen for western blot analysis.

Indices for observation

General status of nude mice, xenograft observation and tumor inhibition rate calculation

The general status including the daily activities, body weight and general status were observed. The long diameter (a) and short diameter (b) of the tumor were measured every two days by a single person using a vernier caliper, and the tumor volume(V) was calculated using the formula $V=ab^2/2$. The

tumors were removed and weighed and the tumor inhibitory rate was calculated using the following formula: tumor inhibitory rate = (1-average tumor weight in tested group/ average tumor weight in negative control group) ×100.

The ultrastructural morphology of the transplanted tumor

The tumor tissue was fixed with 4% glutaraldehyde and then dehydrated with gradient ethanol before embedding the tissue in epoxy resin. The blocks were cut into ultra-thin sections with a microtome. The sections were then stained with saturated uranyl acetate and lead citrate. The ultrastructure of the transplanted tumor was then examined using a JEM-1220 transmission electron microscope.

Impact of ART on cell cycle and apoptosis of tumor cells

Tumor tissues with a size of 1-2 mm^3 were obtained in all transplants from nude mice. The tumors were pressed through a 200-mesh stainless steel screen, and a single cell suspension at a density of 1×10^6/mL was prepared. The cells were then washed three times with PBS and fixed with precooled 75% ethanol and PBS. The cells were treated with 5 μL of PI staining solution and were incubated for 30 min in the dark at 4 ℃. The cells were analyzed by flow cytometry (FCM) to evaluate the cell cycle status and proportion of apoptotic cells using LYSIS software (Becton-Dickinson).

The expression of p53, Bcl-2, Bax and Caspase-3 in transplanted tumor

The expression of p53, Bcl-2, Bax and Caspase-3 in xenografts was detected by Streptavidin/Peroxidase (SP) immunohistochemistry according to the kit instructions. The negative control was performed with PBS instead of primary antibody. The immunoreactivity was evaluated using an immunoreactivity score (IRS), which takes into account both the percentage of positive cells and staining intensity (3). This scoring method avoids the disadvantages of scoring single-positive cells or positive intensity scoring and more accurately reflects the results of immunohistochemical reactions.

The expression of IGF-IR by western blot

To evaluate IGF-IR protein, 0.2 g tissue was removed from liquid nitrogen and washed three times with precooled PBS. The tissue was then mashed into small pieces. The tissue was stirred in 10 volumes of lysis buffer and centrifuged at 4 ℃ for 10 min. The total protein was then isolated. The protein concentration was determined using the Bradford method. The proteins were separated by electrophoresis with sodium dodecyl sulfate-polyacrylamide gel (SDS-PAGE) and then transferred onto polyvinylidene difluoride (PVDF) membranes. After blocking with 5% non-fat dry milk in TBST (20 mM Tris-HCl, 150 mM NaCl and 0.05% Tween-20) for 1 h at room temperature, the membranes were incubated with primary antibodies overnight at 4 ℃. The membranes were then incubated with HRP-conjugated goat anti-rabbit secondary antibodies for 2 h at room temperature. The membranes were washed three times with TBST for 10 min. The specific IGF-IR bands were developed using ECL reagent and imaged using a gel scanner. The protein levels were normalized to GAPDH as a reference.

Statistical analysis

All results were analyzed with SPSS 10.0 software. The data were expressed as means ± standard deviation. The paired *t*-test and χ^2 test were used for statistical analysis between groups. The correlations were evaluated by using the Pearson correlation coefficient. A P value less than 0.05 was considered to be statistically significant.

Results

Effect of ART on tumor growth in nude mice

No mice died during the experiments. The nude mice in the CTX group showed a substantial reduction of appetite, and slow movements and reactions. The food and water intake was not affected in the mice of the other groups. The body weight of the mice in the CTX group was reduced at the conclusion of the experiment. Conversely, the body weights increased in the low and high dose ART groups (*Table 1*).

The ultrastructural morphology of the transplanted tumor

The ultrastructural morphology of the transplanted tumor was observed by transmission electron microscopy. The tumor cells in the NS group exhibited normal ultrastructural morphology and showed an orderly arrangement of cells, regular nuclei, clear nucleolus and normal shape. By contrast, the tumor cells in the ART group were apoptotic, which is characterized by cell shrinkage, plasma membrane blebbing, chromatin condensation with margination of

Table 1 Inhibitory effect of ART on tumor growth in nude mice (mean ± SD, n=5)

Groups	Body weight	Tumor weight	Tumor volume	Inhibition rate (%)
NS	20.37±0.51	0.66±0.13	1.26±0.55	
ART (100 mg/kg)	20.07±0.29	0.50±0.07*	0.73±0.35*	24.39±10.20
ART (200 mg/kg)	19.97±0.12	0.39±0.05*	0.42±0.09**	40.24±7.02
CTX	17.09±1.20*	0.28±0.04*	0.35±0.07**	57.01±5.84
CTX + ART (200 mg/kg)	19.78±1.31	0.21±0.03*	0.31±0.03**	68.29±5.10

*, P<0.05 *vs*. NS group; **, P<0.01 *vs*. NS group; NS, normal saline; ART, artesunate; CTX, cyclophosphamide.

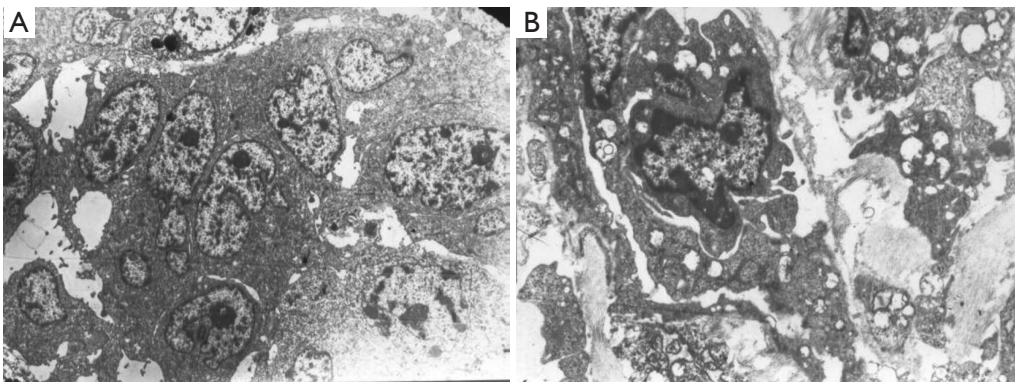

Figure 1 The ultrastructural morphology of the tumors in different groups under transmission electron microscope. (A) Tumor cells of NS group; (B) Tumor cells of ART (100 mg/kg). NS, normal saline; ART, artesunate.

chromatin to the nuclear membrane and formation of apoptotic bodies (*Figure 1*).

The effect of ART on the proliferation and apoptosis of tumor cells

FCM exhibited hypodiploid peaks on the left side of the G1 peak in the FCM histogram (i.e., the apoptosis peak or sub-G1 peak), indicating that ART can induce the apoptosis of the human breast cancer cell line MCF-7 (*Figure 2*). The cells in G_0/G_1 phase increased, and cells in S phase were reduced in the ART group (*Figure 2*).

The effect of ART on the expression of p53, Bcl-2, Bax and Caspase-3 in transplanted tumors

The tumor analysis by immunohistochemistry for Bcl-2 and Bax showed brown stained particles within the cytoplasm and/or the cell membrane in positive cells. Caspase-3 and p53 positive cells showed brown staining in the nucleus.

Bcl-2 was downregulated and the expression of Bax and Caspase-3 was upregulated in the ART treated groups. In addition, the expression of p53, Bcl-2, Bax and Caspase-3 in the ART group was statistically different than the saline group (P<0.05, *Table 2*, *Figure 3*). The correlation analysis showed that BCL-2 was negatively related to Bax (r=–0.490, P=0.043) and Caspase-3 (r=–0.503, P=0.042) expression.

The effect of ART on IGF-IR

The western blot analysis showed a downregulation of IGF-IR in the 100 mg ART and 200 mg ART groups relative to the NS group (*Figure 4*).

Discussion

There is substantial interest in the antitumor effects of ART, which is a water-soluble derivative of ARS. Efferth T *et al*. treated 55 types of human tumor cell lines with ART and found it had an antitumor effect on most tumors (2). The mechanisms of action were related to the induction of apoptosis and anti-angiogenesis properties (5,7,8,15). However, few studies on the anti-tumor effect of ART *in vivo* have been reported. We established a xenograft model

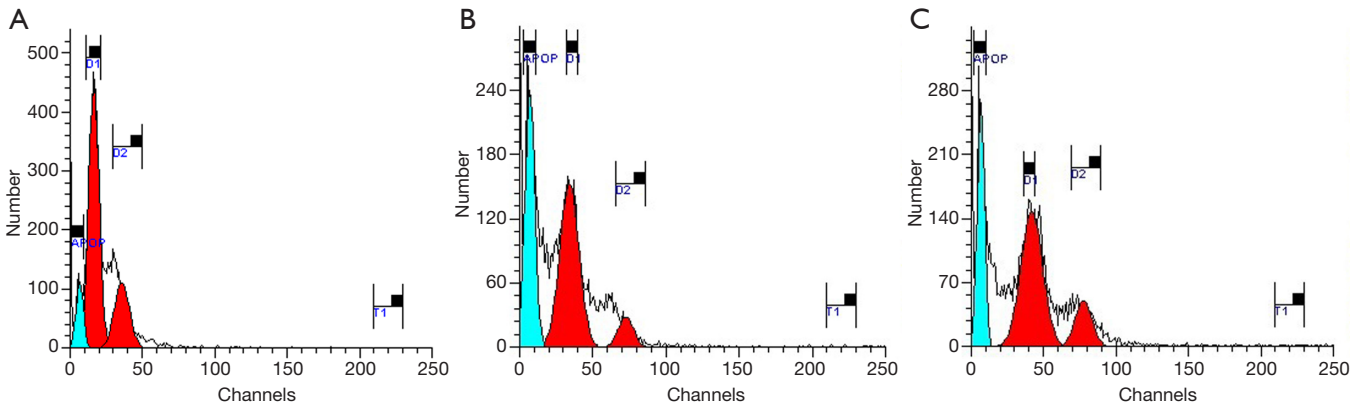

Figure 2 The effects of the drugs on the cell cycle and apoptosis in FCM. (A) NS group; (B) Low dose ART group (100 mg/kg); (C) High dose ART group (200 mg/kg). FCM, flow cytometry; NS, normal saline; ART, artesunate.

Table 2 The effects of ART on the expression of apoptosis related genes in transplanted tumors (mean ± SD, n=5)

Groups	Expression of apoptosis related genes (%)			
	Bcl-2	*Bax*	*Caspase-3*	*p53*
NS	4.58±1.35	1.29±0.81	2.21±0.85	2.73±0.81
100 mg ART	3.01±1.24*	3.53±1.21**	3.25±1.16	2.54±0.75
200 mg ART	1.83±0.69*	4.16±1.13**	4.37±1.32*	2.36±0.61
F	8.211	11.709	4.595	0.539
P	0.006	0.002	0.033	0.624

*, P<0.05 *vs*. NS group; **, P<0.01 *vs*. NS group; ART, artesunate; NS, normal saline.

using the breast tumor cell line MCF-7 by percutaneous injection into nude mice. We then observed the antitumor effect of ART. The general status of mice in the CTX group was poor. However, the general status of the animals was normal in the group receiving combined treatment. This result indicates that ART can decrease the toxic effect of CTX. The animal food and water intake were not affected in the other groups. The tumors with irregular round shape in the control group increased significantly while the tumors in the other groups exhibited a slender round shape. There was a statistically significant difference in the tumor volume for the 100 mg ART, 200 mg ART, CTX and combined treatment group compared to the control group. This result suggests that ART played a role in the treatment of breast cancer. The histopathologic examination showed no damage to vital organs such as heart, liver and kidney, which indicated that ART had no significant toxicity during the experiment. ART has many advantages including specific tumor-targeting without damaging normal cells. Additionally, ART has low toxicity and side effects, which may improve patient quality of life.

Therapies that induce tumor cell apoptosis have become a new treatment for tumors. Tumor apoptosis is also an important index to evaluate for anti-tumor drugs (16). In this study, the induction of apoptosis was observed after treatment with ART. The early morphological changes of apoptosis were observed in the ART group, indicating that ART can induce apoptosis of the transplanted tumor. This result was also demonstrated using FCM, which showed a higher apoptosis rate in the ART group than in the NS group.

The immunohistochemistry showed that apoptosis-related proteins such as p53, Bcl-2, Bax and Caspase-3 in each group have different degrees of expression in transplanted tumor tissue. These results suggest that the activation and inactivation of multiple genes is involved in breast cancer. The expression of Caspase-3 and Bax increased and Bcl-2 decreased significantly in the ART treatment group compared to the control group (P<0.05). This finding indicates that ART induced the apoptosis

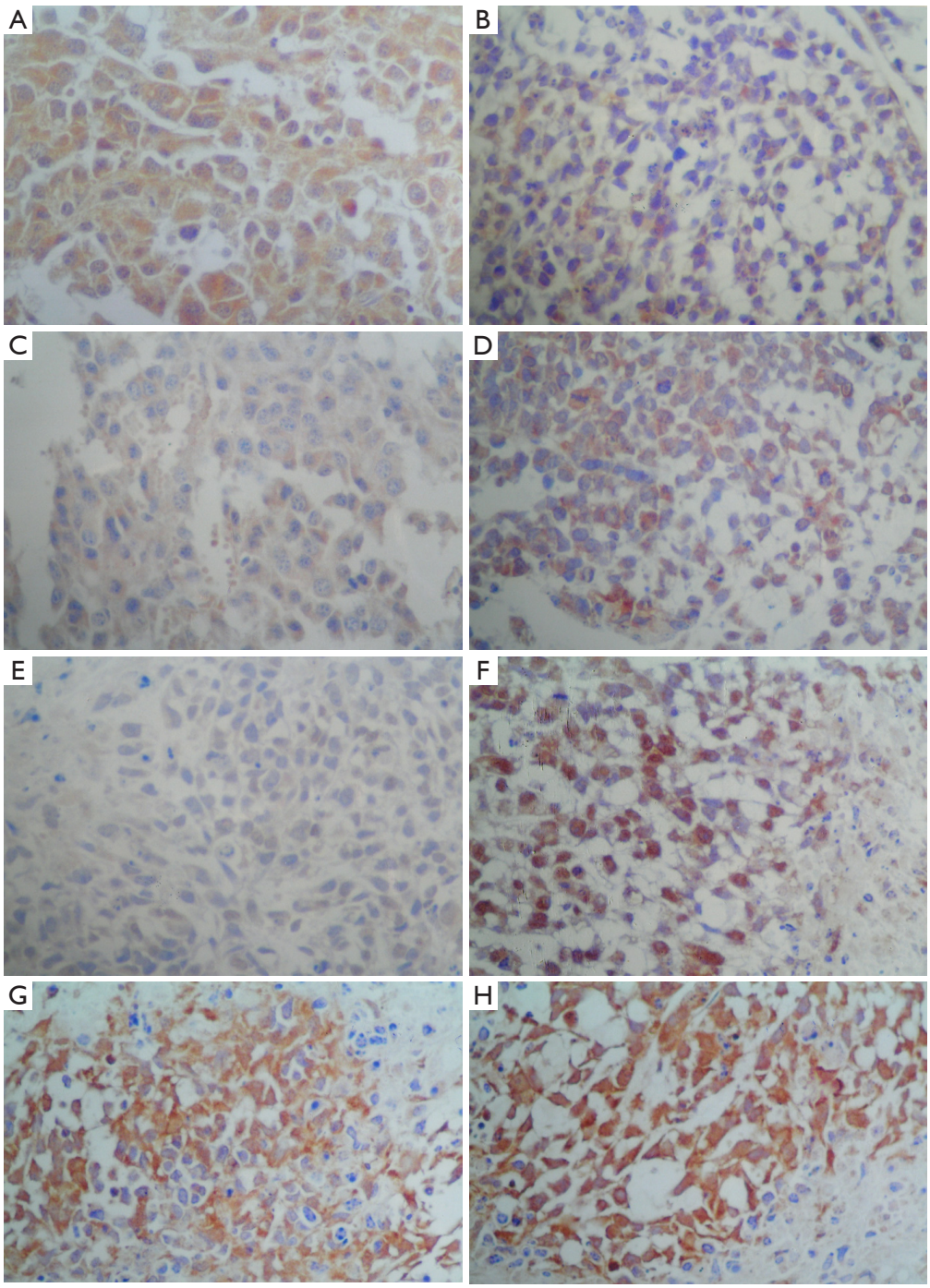

Figure 3 The expression of Bcl-2, Bax, p53 and caspase-3 in the transplanted tumors (400×). (A) Bcl-2 expression in NS group; (B) Bcl-2 expression in high dose ART group (200 mg/kg); (C) Bax expression in NS group; (D) Bax expression in high dose ART group (200 mg/kg); (E) Caspase-3 expression in NS group; (F) Caspase-3 expression in high dose ART group (200 mg/kg); (G) p53 expression in NS group; (H) p53 expression in high dose ART group (200 mg/kg). NS, normal saline; ART, artesunate.

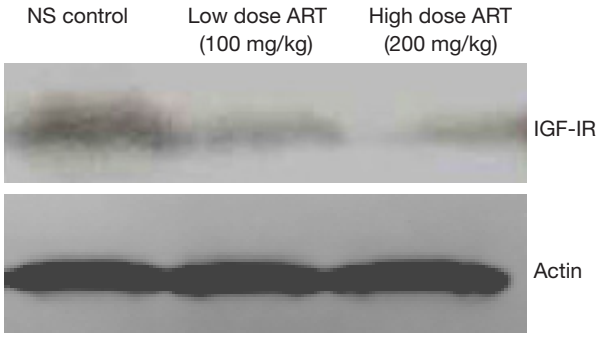

Figure 4 The expression of IGF-IR in the transplanted tumor in Western blot. NS, normal saline; ART, artesunate; IGF-IR, insulin-like growth factor-I receptor.

of breast tumor cells by inhibiting the expression of the anti-apoptosis gene *Bcl-2* and improving the expression of apoptotic genes *Bax* and *Caspase-3*. The correlation analysis showed that *Bcl-2* had a significant negative relationship with *Bax* and *Caspase-3*, indicating that these genes contribute to tumor cell apoptosis. There was no significant difference detected in the expression of p53 between the treatment group and the control group. This finding is consistent with the reports of Zhang X (17) and Efferth T *et al.* (18), who reported that the induction of apoptosis mediated by ART was not p53-dependent.

IGF-IR plays a regulatory role in cell division, differentiation and proliferation. The IGF-IR pathway promotes the proliferation of cells and causes malignant transformation of cells and inhibits tumor cell apoptosis. These functions may be associated with the apoptosis-suppressing gene *Bcl-2*. In the current study, western blot analysis showed that the expression of IGF-IR was downregulated by ART. However, further study is needed to investigate its role in the regulation of apoptosis by IGF-IR and other factors.

In conclusion, as an anticancer treatment ART has the advantages of low toxicity and side effects with a remarkable anticancer effect. These findings suggest that ART may have wide therapeutic application in the treatment of tumors.

Acknowledgements

Funding: Province Science Fund for Young Scholars (No. QC05C46); Science Foundation from Health Bureau of Heilongjiang Province (No. 2005-47).
Disclosure: The authors declare no conflict of interest.

References

1. White NJ. Qinghaosu (artemisinin): the price of success. Science 2008;320:330-4.
2. Efferth T, Dunstan H, Sauerbrey A, et al. The anti-malarial artesunate is also active against cancer. Int J Oncol 2001;18:767-73.
3. Efferth T, Sauerbrey A, Olbrich A, et al. Molecular modes of action of artesunate in tumor cell lines. Mol Pharmacol 2003;64:382-94.
4. Lai H, Sasaki T, Singh NP, et al. Effects of artemisinin-tagged holotransferrin on cancer cells. Life Sci 2005;76:1267-79.
5. Singh NP, Lai HC. Artemisinin induces apoptosis in human cancer cells. Anticancer Res 2004;24:2277-80.
6. Lu JJ, Meng LH, Cai YJ, et al. Dihydroartemisinin induces apoptosis in HL-60 leukemia cells dependent of iron and p38 mitogen-activated protein kinase activation but independent of reactive oxygen species. Cancer Biol Ther 2008;7:1017-23.
7. Jiao Y, Ge CM, Meng QH, et al. Dihydroartemisinin is an inhibitor of ovarian cancer cell growth. Acta Pharmacol Sin 2007;28:1045-56.
8. Chen T, Li M, Zhang R, et al. Dihydroartemisinin induces apoptosis and sensitizes human ovarian cancer cells to carboplatin therapy. J Cell Mol Med 2009;13:1358-70.
9. Li LN, Zhang HD, Yuan SJ, et al. Artesunate attenuates the growth of human colorectal carcinoma and inhibits hyperactive Wnt/beta-catenin pathway. Int J Cancer 2007;121:1360-5.
10. Dong HY, Song WH, Sun JP, et al. Effect of artemisinin on the growth of Hela. Journal of Harbin Medical University 2002;36:423-4.
11. Dong HY, Wang ZF, Song WH, et al. Apoptosis induced by artemisinin in K562 cells. Bulletin of China Cancer 2003:12:473-5.
12. Lai H, Singh NP. Selective cancer cell cytotoxicity from exposure to dihydroartemisinin and holotransferrin. Cancer Lett 1995;91:41-6.
13. Efferth T, Olbrich A, Bauer R. mRNA expression profiles for the response of human tumor cell lines to the antimalarial drugs artesunate, arteether, and artemether. Biochem Pharmacol 2002 ;64:617-23.
14. Li Y, Shan F, Wu JM, et al. Novel antitumor artemisinin derivatives targeting G1 phase of the cell cycle. Bioorg Med Chem Lett 2001;11:5-8.
15. Chen HH, Zhou HJ, Fang X. Inhibition of human cancer

cell line growth and human umbilical vein endothelial cell angiogenesis by artemisinin derivatives in vitro. Pharmacol Res 2003;48:231-6.
16. Reed JC. Apoptosis-targeted therapies for cancer. Cancer Cell 2003;3:17-22.
17. Zhang X, Yang X, Pan Q. Artesunate's effect of anticancer and apoptosis induction in human liver tumor (BEL-7402). Chinese Traditional and Herbal Drugs 1998;29:467-9.
18. Efferth T, Benakis A, Romero MR, et al. Enhancement of cytotoxicity of artemisinins toward cancer cells by ferrous iron. Free Radic Biol Med 2004;37:998-1009.

Cite this article as: Dong HY, Wang ZF. Antitumor effects of artesunate on human breast carcinoma MCF-7 cells and IGF-IR expression in nude mice xenografts. Chin J Cancer Res 2014;26(2):200-207. doi: 10.3978/j.issn.1000-9604.2014.04.07

